Elsevier Editorial System(tm) for Applied Mathematical Modelling

Manuscript Draft

Manuscript Number: APM-D-16-00732R1

Title: Modelling functionally graded materials in heat transfer and thermal stress analysis by means of graded finite elements

Article Type: Research Paper

Keywords: functionally graded materials; graded finite element; heat transfer analysis; thermal stresses.

Corresponding Author: Dr. Vyacheslav Nikolayevich Burlayenko, Ph.D.

Corresponding Author's Institution: National Technical University 'Kharkiv Polytechnic Institute'

First Author: Vyacheslav Nikolayevich Burlayenko, Ph.D.

Order of Authors: Vyacheslav Nikolayevich Burlayenko, Ph.D.; Holm Altenbach, Prof. Dr.-Ing. habil.; Tomasz Sadowski, Prof. D.Sc. ; Svetlana Dimitrova , Assistant Prof. MMath. ; Atul Bhaskar, Professor PhD

Abstract: For better understanding of the behavior of functionally graded materials (FGM) in high temperature environment, a reliable and efficient numerical tool is required for predictions of heat transfer behavior and thermally-induced stresses in them. This study presents a finite element formulation of a coupled thermo-mechanical problem in functionally graded metal/ceramic plates. The theoretical framework considers the finite element method (FEM) which is applied to the development of a functionally graded two-dimensional plane strain finite element. The plane strain graded finite element is incorporated within the ABAQUS tm code via the combination of user-defined subroutines. The subroutines enable us to program graded mechanical and thermal properties of the FGM as continuous position-dependent functions and, then, to sample them directly at the Gauss integration points of the element. The performance of the developed graded finite element is verified by comparisons with results known in the literature and with calculated using conventional homogeneous elements in a layered model. The solutions of thermo-mechanical problems of functionally graded plates referring to pure mechanical and thermal tasks, and uncoupled and coupled analyses of thermoelasticity are carried out and discussed in the paper.

Highlights

• A finite element formulation of the coupled thermo-mechanical problem of a FGM plate is presented.

• A graded plain strain element is incorporated within the ABAQUS code environment.

• The performance of the graded element is validated by solving thermo-mechanical problems.

• The examples reveal a high accuracy and efficiency of the developed graded finite element.

Modelling functionally graded materials in heat transfer and thermal stress analysis by means of graded finite elements

V.N. Burlayenko[*,a,b], H. Altenbach[c], T. Sadowski[d], S.D. Dimitrova[a], A. Bhaskar[b]

[a]*Department of Applied Mathematics, National Technical University 'KhPI', 21 Frunze Str., Kharkiv 61002, Ukraine*
[b]*Faculty of Engineering and the Environment, University of Southampton, Southampton SO16 7QF, UK*
[c]*Institute of Mechanics, Otto-von-Guerike University of Magdeburg, 2 Universitätsplatz, Magdeburg 39106, Germany*
[d]*Department of Solid Mechanics, Lublin University of Technology, 40 Nadbystrzycka Str., Lublin 20-618, Poland*

Abstract

For better understanding of the behavior of functionally graded materials (FGM) in high temperature environment, a reliable and efficient numerical tool is required for predictions of heat transfer behavior and thermally-induced stresses in them. This study presents a finite element formulation of a coupled thermo-mechanical problem in functionally graded metal/ceramic plates. The theoretical framework considers the finite element method (FEM) which is applied to the development of a functionally graded two-dimensional plane strain finite element. The plane strain graded finite element is incorporated within the ABAQUS™ code via the combination of user-defined subroutines. The subroutines enable us to program graded mechanical and thermal properties of the FGM as continuous position-dependent functions and, then, to sample them directly at the Gauss integration points of the element. The performance of the developed graded finite element is verified by comparisons with results known in the literature and with calculated using conventional homogeneous elements in a layered model. The solutions of thermo-mechanical problems of functionally graded plates referring to pure mechanical and thermal tasks, and uncoupled and coupled analyses of thermoelasticity are carried out and discussed in the paper.

Key words: functionally graded material, graded finite element, heat transfer, thermal stresses

1. Introduction

Functionally graded materials (FGMs), originally developed as thermal barrier coatings for aerospace structures and fusion reactors have nowadays received a wide spread as structural components in transportation, energy, electronics and biomedical engineering for the general use in the high temperature environment [1]. One of typical FGMs are functionally graded metal/ceramic composites which offer optimal thermo-mechanical characteristics, also they allow one to avoid interfacial delamination usual for layered compositions of a ceramic coating and a metal substrate [2]. The behaviour of FGMs including heat transfer problems and thermal stress analyses in metal/ceramic FGMs have been extensively studied in the past decade, e.g. [3, 4] among many others. However, to respond to demands of new structures and technologies connected with further increasing the in-service temperature, the thermal behaviour and efficiency of FGMs should be better understood. The primary interest of this, in essence, is the examination of the thermally-induced stresses that have a critical relevance to fracture mechanisms in FGM structural elements [5, 6, 7]. Therefore, it is of huge importance to have reliable and efficient computational models for evaluating complex thermo-mechanical response of FGM structures at a design stage.

A comprehensive review of the principal theoretical developments in functionally graded materials with an emphasis on studies on heat transfer issues, stress, stability, dynamic and fracture analyses, testing, manufacturing, design and applications has been reported in [8]. From this review, it is obvious that heat transfer and thermal stress analysis of FGM is analytically complicated to be performed, as a result the closed-form solution of these problems is possible only for few cases with particular types of thermal loads, boundary conditions and inhomogeneity. Although it is worth mentioning that direct approaches based on the original idea of Cosserat possess a high potential to analytical predictions of thermo-mechanical response in FGMs as shown in [9], where a functionally graded plate was successfully analyzed. Nevertheless, in general, closed-form solutions are difficult, if not impossible, to be found for FGM plates of finite dimensions and where the material properties vary in patterns other than exponentially. Hence the numerical solutions are most suitable for these types of problems. In this regard, the finite element method (FEM) is a power tool for solving various multi-disciplinary problems of mechanics including the thermal and mechanical problems in FGMs.

The main issue encountered in using FEM in FGMs is concerned with modeling continuously varying material properties.

[*]Corresponding author
Email addresses: burlayenko@kpi.kharkov.ua, V.Burlayenko@soton.ac.uk (V.N. Burlayenko), holm.altenbach@ovgu.de (H. Altenbach), t.sadowski@pollub.pl (T. Sadowski), s.dimitrova@kpi.kharkov.ua (S.D. Dimitrova), A.Bhaskar@soton.ac.uk (A. Bhaskar)

The simplest way to model a graded material inhomogeneity involves the use of conventional homogeneous elements in successive layers of the mesh, containing own material properties. This leads to a stepwise change in properties along the direction of material gradient. Such models have been already used by a number of researchers, e.g. in [10, 11, 12] and they produced reasonable results. However this approach requires a fine mesh to achieve the accuracy, in turn, it leads to excessive computational costs. Moreover, the preparation of input data and adjusting the mesh of different gradation regions is quite cumbersome in this approach as well. Thereby, it is important to include the gradient of material properties into the model at the element level so that the accuracy would be retained when coarser meshes are used. Recently such finite elements (FE), called as graded finite elements have been developed and applied for solving some problems involving FGMs. Authors in [13] proposed a 2-D graded finite element with material properties evaluated directly at the Gauss points. An alternative graded element was developed in [14], a fully isoparametric element formulation that interpolates material properties at each Gauss point from the nodal values, using the same shape functions as the displacements was proposed there. In [15], authors studied thermal stresses due to uniform temperature change in a FGM coating using graded elements, where inhomogeneity was specified at the Gauss points. The transient heat transfer analysis of FGMs using adaptive precise time integration and isometric graded finite elements was carried out in [16].

Although commercially available finite element codes have become popular among engineers and researchers due to their versatility, sufficient accuracy and their ease in use, they pose a challenge to implement variations of material properties in FE models. In [17] authors proposed an original way to assign material gradients within the ANSYS code. They provided the FE model with an initial temperature distribution that matches the desired temperature-dependent material properties. It allowed them to examine a fracture problem in a FGM plate. However this technique is not suitable for thermo-mechanical analyses. In [18] the authors have used the ABAQUS software to calculate the crack-tip field in a cracked FGM plate under mechanical loading. To assign a variation of material properties to the FE model, authors programmed a mechanical law within the user-defined subroutine UMAT. The same approach for developing a graded element has been reported in [19], where the authors applied that element for analysing the pavement behaviour. Moreover, the authors showed that graded element gives a far greater modelling accuracy in comparison with a homogeneous element for a FGM plate under a mechanical load. The same engineering package has also been used for solving heat conduction problems in simple FGM structures in [20]. The authors incorporated gradually varying thermal properties into finite element models of the FGM structures using the user-defined subroutine UMATHT available in ABAQUS for thermal analyses. In [21] the analysis of heat transfer and thermal stresses in metal/ceramic thermal barrier coatings of turbine blades has been carried out using the abilities of the both numerical packages mentioned above, but graded finite elements were not used. The numerical results and analytical solutions on distributions of the temperature and thermally-induced stresses in a FGM plate under thermal shock loading have been obtained in [23]. Those calculations were carried out using the ABAQUS code, where material gradients were programmed by using a combination of mechanical and thermal subroutines of this package. The same user-defined subroutines have been employed by the authors in [24] to carry out the crack propagation analysis with the XFEM approach available in ABAQUS for a FGM strip under thermal shock. More recently in [25] the same authors applied this modelling technique for computing the thermal stress intensity factor in the FGM strip. Also the XFEM has been used for analyzing transient thermal shock fracture of functionally graded piezoelectric materials in [26]. The authors in [27] have studied a quasi-static fracture of FGM plates. They modelled the crack growth in plates subjected to mechanical loads by using the XFEM within ABAQUS. In that research, the implementation of material gradients into the models of plates has been achieved by programming the material properties as functions of selected field variables within the USDFLD subroutine instead of using the material user-defined routines. Thermal cracking of a FGM plate undergoing thermal shock has been examined in [28, 29]. The authors employed the virtual crack propagation technique available in ABAQUS that had been applied to fracture analysis of laminated composites in [30] to simulate the crack growth in the FGM plate. They incorporated gradients of thermal and mechanical properties of the plate into the model via the combination of subroutines mentioned above. This allowed them to take into account gradual variations of the Poisson's coefficient and the mass density in the calculations that has not been done in the previous works.

The literature search showed that the FEM is intensively exploited for analyzing heat transfer and mechanical problems including fracture in FGM structures. However, to the best of our knowledge, most of publications, where the FEM is used as a research tool for FGMs, usually skip the description of the finite element statement underlying for incorporating gradients of material properties into the finite element model. Although such theoretical derivations are needed to eliminate the gap between the traditional finite element theory based on homogeneous elements and the finite element framework involving graded finite elements. Some theoretical descriptions of graded elements existing in the literature do not include simultaneously the thermal and mechanical statements in FGMs. Thereby, the main goal of the present paper is the formulation of a theoretical framework to develop a graded finite element which can be applied for a coupled thermo-mechanical analysis of FGM plates. It is intended to consider the basic equations of a two-dimensional (2-D) thermo-mechanical problem of FGMs, for which the finite element approximation is being developed. A plane strain graded finite element elaborated with this finite element framework within the ABAQUS/Standard code [31] demonstrates its potential for accurate and robust predictions of thermo-mechanical problems in FGM plates. The combination of the user-defined subroutines UMAT, UMATHT and USDFLD is used to implement graded material properties into the finite element model. The verification of the element is per-

formed and advantages of its using for heat transfer and stress analyses of metal/ceramic graded plates are demonstrated.

2. General statement of thermo-mechanical problem

The local system of partial differential equations governing the coupled thermo-mechanical problem for a body made of a functionally graded material is presented first. Let a set of material points $\mathbf{X}$ of a continuously inhomogeneous isotropic body occupy a 2-D domain, which consists of the material area $\mathcal{A}_0 \in \mathbb{R}^2$ and its bounded line $\Gamma_0 \in \mathbb{R}^2$. In the Lagrangian description, the coupled initial-boundary value problem of linear thermoelasticity at each spatial point $\mathbf{x}(\mathbf{X}, t)$ of the domain $\mathcal{A}$ at the time instant t can be expressed as [32]:

$$\sigma_{ji,j} + b_i = \rho(\mathbf{x})\ddot{u}_i \tag{1}$$

$$-q_{i,i} = \rho(\mathbf{x})c_v(\mathbf{x})\dot{\theta} + T_0\beta(\mathbf{x})\dot{u}_{k,k} - \mathcal{R}, \tag{2}$$

where σ_{ij} stands for the components of the Cauchy stress tensor, u_i represents the components of a displacement, $\theta(\mathbf{x}, t) = T - T_0$ denotes a temperature change of the instantaneous absolute temperature $T(\mathbf{x}, t)$ above the uniform reference temperature T_0, and dots denote differentiation with respect to time. Also the symbols q_i and b_i indicate the components of a surface heat flux and body forces, respectively, and $\mathcal{R}$ is an internal heat source. Material parameters such as the mass density $\rho(\mathbf{x})$, the specific heat $c_v(\mathbf{x})$ and the stress-temperature modulus $\beta(\mathbf{x})$ are functions of a spatial position $\mathbf{x} = (x, y)$ in the Cartesian coordinate system.

Assuming small displacements and small strains, we do not distinguish between the material placements $\mathbf{X}$ and the current placements $\mathbf{x}$. Herewith, the total infinitesimal strains ε_{ij} at each point $\mathbf{x}$ of the domain $\mathcal{A}$ can be decomposed into elastic strains ε_{ij}^{el} and thermal strains ε_{ij}^{th} caused by a temperature change as follows:

$$\varepsilon_{ij} = \frac{1}{2}(u_{i,j} + u_{j,i}) = \varepsilon_{ij}^{el} + \varepsilon_{ij}^{th} \tag{3}$$

$$\varepsilon_{ij}^{th} = \alpha(\mathbf{x})\delta_{ij}\theta, \tag{4}$$

where $\alpha(\mathbf{x})$ is the coefficient of thermal expansion and δ_{ij} is the Kronecker delta.

Since only linear material behaviour is considered, the components of the stress tensor in (1) satisfy the Duhamel-Neumann relations, which for an isotropic inhomogeneous material can be expressed as:

$$\sigma_{ij} = \lambda(\mathbf{x})\varepsilon_{kk}\delta_{ij} + 2\mu(\mathbf{x})\varepsilon_{ij} - \beta(\mathbf{x})\delta_{ij}\theta. \tag{5}$$

Following the thermodynamic assumptions outlined in [32] the heat conduction in the energy equation (2) is governed by Fourier's law which in the case of the isotropic inhomogeneous material can be written in the form:

$$q_i = -\kappa(\mathbf{x})\theta_{,i}. \tag{6}$$

Here the Lamé constants $\lambda(\mathbf{x})$ and $\mu(\mathbf{x})$, the thermal conductivity $\kappa(\mathbf{x})$ and the coefficient of thermal expansion $\alpha(\mathbf{x})$ such that $\beta = \alpha(3\lambda + 2\mu)$ are pointwise functions of location.

Analyzing the system of (1) and (2) one can see that the coupling between deformation and temperature fields exists. The temperature terms occur in the equations of motion, while the rate of the dilatation of deformations is presented in the energy equation. Hence, the system of equations (1)-(6) must be solved simultaneously for the displacements $u_i(\mathbf{x}, t)$ and the temperature field $\theta(\mathbf{x}, t)$. In doing so, proper initial and boundary conditions for mechanical and thermal fields should be adopted.

The combination of initial conditions for a mechanical problem can be expressed by the following equations:

$$\begin{aligned} u_i(\mathbf{x}, 0) &= u_0(\mathbf{x}), \\ \dot{u}_i(\mathbf{x}, 0) &= v_0(\mathbf{x}) \end{aligned} \tag{7}$$

and the boundary conditions

$$\begin{aligned} u_i &= \bar{u}_i \quad \text{on} \quad \Gamma_u \quad \text{and} \quad t > 0 \\ \sigma_{ij}n_j &= \bar{t}_i \quad \text{on} \quad \Gamma_\sigma \quad \text{and} \quad t > 0 \end{aligned} \tag{8}$$

where u_0 and v_0 are displacements and velocities at the initial instant of time, and $\bar{t}_i$ and $\bar{u}_i$ are prescribed traction and displacements, respectively, given on the parts of the closed line $\Gamma = \Gamma_\sigma \cup \Gamma_u$ with the unit outward normal vector n_i.

Thermal conditions are specified at an initial instant of time as initial temperature:

$$T(\mathbf{x}, 0) = T_0(\mathbf{x}) \tag{9}$$

and at any instant of time as prescribed temperature $\bar{T}(\mathbf{x}, t)$, prescribed heat flux $\bar{q}(\mathbf{x}, t)$ per unit boundary and prescribed heat flux $\mathcal{R}(\mathbf{x}, t)$ per unit domain, and convection in the form:

$$\begin{aligned} T(\mathbf{x}, t) &= \bar{T} \quad \text{on} \quad \Gamma_T \quad \text{and} \quad t > 0 \\ q_i n_i &= \bar{q} \quad \text{on} \quad \Gamma_{q_1} \quad \text{and} \quad t > 0 \\ q_i n_i &= h(T - T_\infty) \quad \text{on} \quad \Gamma_{q_2} \quad \text{and} \quad t > 0 \end{aligned} \tag{10}$$

where $h = h(\mathbf{x}, t)$ is the heat film transfer coefficient, T_∞ is a temperature of a surrounding medium, and $\Gamma_T \cup \Gamma_{q_1} \cup \Gamma_{q_2} = \Gamma$.

3. Material properties

The problem stated above can be applied without loss of generality to functionally graded metal/ceramic plates such as that shown in Fig. 1. It is worth to notice that all material properties of the plate vary smoothly along the thickness of the FGM and those distributions are assumed to be known.

The thermo-mechanical analysis of a FGM plate under thermal and/or mechanical loadings is discussed from the macroscopic standpoint, i.e. by evaluating macroscopic stress components induced in the FGM plate due to a temperature gradient. To accurately model a temperature field and stress distributions in a FGM plate, a proper estimate of thermal and mechanical properties in the inhomogeneous material is required.

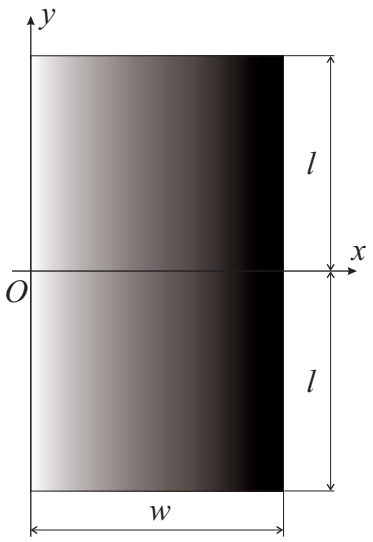

Figure 1: Schematic diagram of a functionally graded rectangular plate.

In this work, we assume that the plate consists of particles of titanium alloy Ti-6Al-4V and zirconium dioxide ZrO_2 ceramic. The effective material characteristics of the studied functionally graded Ti-6Al-4V/ZiO_2 plate can be found in [12]. The authors suggested there that the volume fraction of the metal phase through the plate width (Fig. 1) varies in accordance with a power function law:

$$V_m = \left(\frac{x}{w}\right)^p, \tag{11}$$

where w is a width of plate in Fig. 1.

Then the volume fraction of the ceramic phase is calculated as $V_c = 1 - V_m$. Here and in what follows the subscripts c and m of the material parameters denote the ceramic and metal phases, respectively. From (11) it follows that the FGM is ceramic rich when the parameter $p > 1$ and metal rich when the parameter $p < 1$. Fig. 2 shows the volume fraction variation of the metal phase along the plate width w for various values of the power coefficient p.

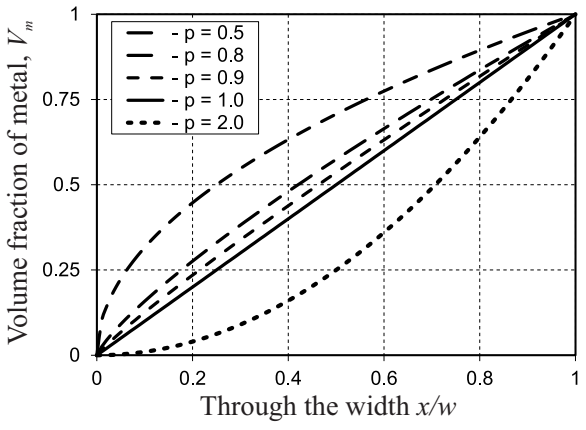

Figure 2: Compositional profiles of the functionally graded material.

Table 1: Material properties of Ti-6Al-4V and ZiO_2 [12].

Property	Constituents	
	Ceramic ZiO_2	Metal Ti-6Al-4V
Young's modulus E, [GPa]	117	66.2
Poisson's ratio ν	0.333	0.32
Mass density ρ, [kg/m^3]	5600	4420
Coefficient of thermal expansion α, 10^{-6} [1/K]	7.11	10.3
Thermal conductivity κ, [W/(mK)]	2.036	18.1
Specific heat c_ε, [J/(kgK)]	615.6	808.3

The variations of the thermo-mechanical properties of the FGM plate, shown in Fig. 1, in the direction of the $x-$coordinate with negligible porosity are defined by means of the rule of mixtures of a two-phase material as follows:

$$\begin{aligned}
E(\mathbf{x}) &= E_c\left\{\frac{E_c + (E_m - E_c)V_m^{2/3}}{E_c + (E_m - E_c)(V_m^{2/3} - V_m)}\right\}\\
\nu(\mathbf{x}) &= \nu_m V_m + \nu_c V_c\\
\rho(\mathbf{x}) &= \rho_m V_m + \rho_c V_c\\
\alpha(\mathbf{x}) &= \frac{\alpha_m V_m E_m/(1-\nu_m) + \alpha_c V_c E_c/(1-\nu_c)}{V_m E_m/(1-\nu_m) + V_c E_c/(1-\nu_c)}\\
\kappa(\mathbf{x}) &= \kappa_c\left\{\frac{1 + 3(\kappa_m - \kappa_c)V_m}{3\kappa_c + (\kappa_m - \kappa_c)V_c}\right\}\\
c_\upsilon(\mathbf{x}) &= \frac{c_m\rho_m V_m + c_c\rho_c V_c}{\rho_m V_m + \rho_c V_c},
\end{aligned} \tag{12}$$

where E,ν, ρ, α, κ and c_υ stand for Young's modulus, Poisson's ratio, mass density, coefficient of linear thermal expansion, thermal conductivity and specific heat, respectively, and they are spatially-dependent functions.

The mechanical and thermophysical properties of the constituents of the functionally graded material at a reference temperature of 1000K are taken as those in [12] and are listed in Table 1.

For the sake of simplicity, the mechanical and thermal constants are assumed to be independent of the temperature in the following simulations.

4. Finite element formulation

The weak form of the differential equations of motion (1) and the local energy balance equation (2) can be written as follows:

$$\begin{aligned}
\int_{\mathcal{A}} \frac{\partial(\delta u_i)}{\partial x_j}\sigma_{ij}d\mathcal{A} - \int_\Gamma \delta u_i \bar{t}_i d\Gamma - \int_{\mathcal{A}} \delta u_i b_i d\mathcal{A} + \\
\int_{\mathcal{A}} \delta u_i \rho(\mathbf{x})\ddot{u}_i d\mathcal{A} = 0, \quad \forall \delta u_i \in \mathcal{U}
\end{aligned} \tag{13}$$

and

$$\int_{\mathcal{A}} \delta\theta\rho(\mathbf{x})c_v(\mathbf{x})\frac{\partial\theta}{\partial t}d\mathcal{A} - \int_{\mathcal{A}} \frac{\partial(\delta\theta)}{\partial x_i}q_i d\mathcal{A} + \int_{\Gamma} \delta\theta\bar{q}d\Gamma + \int_{\mathcal{A}} \delta\theta T_0\beta(\mathbf{x})\frac{\partial u_{k,k}}{\partial t}d\mathcal{A} - \int_{\mathcal{A}} \delta\theta\mathcal{R}d\mathcal{A} = 0, \quad \forall\delta\theta \in \mathcal{T}, \tag{14}$$

where kinematically admissible virtual displacements δu_i and admissible virtual temperature field $\delta\theta$, obeying the essential boundary conditions reside in appropriate vector spaces $\mathcal{U}$ and $\mathcal{T}$. The system of the variational equations (13) and (14) presents a variational statement of the fully coupled thermo-mechanical problem which is suitable to be solved by means of the FEM.

The finite element formulation of the variational problem is obtained by discretizing the solution domain into a number of arbitrary non-overlapping finite elements such that $\mathcal{A}_0 = \bigcup_{e=1}^{Ne} \mathcal{A}_0^{(e)}$. In each base element $\mathcal{A}^{(e)}$ at a time t, the components of the displacement vector and the temperature change are approximated by suitable interpolation functions as follows:

$$u_i^{(e)}(\mathbf{x}, t) = N^I(\mathbf{x})U_i^I(t) \tag{15}$$

$$\theta^{(e)}(\mathbf{x}, t) = \tilde{N}^P(\mathbf{x})\Theta^P(t) \tag{16}$$

where $I, P = 1, 2, \ldots n^{(e)}$ are nodal points and $n^{(e)}$ is a number of nodes in the base element, $N^I(\mathbf{x})$ and $\tilde{N}^P(\mathbf{x})$ are shape functions for the displacements and the temperature field, accordingly, associated with correspondent nodes I and P, and $U_i^I(t)$ and $\Theta^P(t)$ are nodal unknown displacements and temperature, respectively. Herein, the summation over the repeated indices I and P is used.

In accordance with the Galerkin method, the variational fields of the displacements δu_i and the temperature $\delta\theta$ residing in finite-dimensional vector spaces $\mathcal{U}^h$ and $\mathcal{T}^h$, which are subsets of the corresponding infinite counterparts, are interpolated by the same functions as in (15) and (16), respectively. Substituting the approximations (15) and (16) and associated with them variations into the functionals (13) and (14), accounting for the constitutive equations for the stress tensor (5) and the surface heat flux (6), the finite element equations of the coupled thermo-mechanical problem take the form:

$$\left(\int_{\mathcal{A}^{(e)}} \rho\, N^I N^J d\mathcal{A}\right)\ddot{U}_i^J + \left(\int_{\mathcal{A}^{(e)}} \lambda\frac{\partial N^I}{\partial x_i}\frac{\partial N^J}{\partial x_j}d\mathcal{A}\right)U_j^J + \left(\int_{\mathcal{A}^{(e)}} \mu\frac{\partial N^I}{\partial x_j}\frac{\partial N^J}{\partial x_i}d\mathcal{A}\right)U_j^J + \left(\int_{\mathcal{A}^{(e)}} \mu\frac{\partial N^I}{\partial x_j}\frac{\partial N^J}{\partial x_j}d\mathcal{A}\right)U_i^J - \underline{\left(\int_{\mathcal{A}^{(e)}} \beta\frac{\partial N^I}{\partial x_i}\tilde{N}^Q d\mathcal{A}\right)\Theta^Q} = \int_{\mathcal{A}^{(e)}} b_i N^I d\mathcal{A} + \int_{\Gamma^{(e)}} \bar{t}_i N^I d\Gamma, \tag{17}$$

and

$$\left(\int_{\mathcal{A}^{(e)}} \rho c_v\tilde{N}^P\tilde{N}^Q d\mathcal{A}\right)\dot{\Theta}^Q + \left(\int_{\mathcal{A}^{(e)}} \kappa\frac{\partial\tilde{N}^P}{\partial x_i}\frac{\partial\tilde{N}^Q}{\partial x_i}d\mathcal{A}\right)\Theta^Q + \underline{\left(\int_{\mathcal{A}^{(e)}} T_0\beta\tilde{N}^P\frac{\partial N^J}{\partial x_i}d\mathcal{A}\right)\dot{U}_i^J} = \int_{\mathcal{A}^{(e)}} \mathcal{R}\tilde{N}^P d\mathcal{A} + \int_{\Gamma^{(e)}} \bar{q}\tilde{N}^P d\Gamma, \tag{18}$$

where $I, J, P, Q = 1, \ldots, n^{(e)}$ and $i, j = 1, 2$. The underlined terms point out the coupling between the mechanical and thermal equations, i.e. the mechanical equation (17) contains the thermal strains, whereas the dilatation of strains contributes in the thermal equation (18).

In matrix notations the expressions presented above can be rewritten as follows:

$$\begin{bmatrix} \mathbf{M}_{uu}^{(e)} & \mathbf{0} \\ \mathbf{0} & \mathbf{0} \end{bmatrix}\begin{Bmatrix} \ddot{\mathbf{U}}^{(e)} \\ \ddot{\Theta}^{(e)} \end{Bmatrix} + \begin{bmatrix} \mathbf{0} & \mathbf{0} \\ \mathbf{C}_{\theta u}^{(e)} & \mathbf{C}_{\theta\theta}^{(e)} \end{bmatrix}\begin{Bmatrix} \dot{\mathbf{U}}^{(e)} \\ \dot{\Theta}^{(e)} \end{Bmatrix} + \begin{bmatrix} \mathbf{K}_{uu}^{(e)} & \mathbf{K}_{u\theta}^{(e)} \\ \mathbf{0} & \mathbf{K}_{\theta\theta}^{(e)} \end{bmatrix}\begin{Bmatrix} \mathbf{U}^{(e)} \\ \Theta^{(e)} \end{Bmatrix} = \begin{Bmatrix} \mathbf{F}_u^{(e)} \\ \mathbf{F}_\theta^{(e)} \end{Bmatrix} \tag{19}$$

Here the matrices are presented in Appendix.

Using the assembly procedure $(\bullet) = \mathbb{A}_{e=1}^{Ne}(\circ)^{(e)}$, where the symbol $\mathbb{A}$ represents the assembly operator over all finite elements. The global semi-discrete finite element equation reads

$$\begin{bmatrix} \mathbf{M}_{uu} & \mathbf{0} \\ \mathbf{0} & \mathbf{0} \end{bmatrix}\begin{Bmatrix} \ddot{\mathbf{U}} \\ \ddot{\Theta} \end{Bmatrix} + \begin{bmatrix} \mathbf{0} & \mathbf{0} \\ \mathbf{C}_{\theta u} & \mathbf{C}_{\theta\theta} \end{bmatrix}\begin{Bmatrix} \dot{\mathbf{U}} \\ \dot{\Theta} \end{Bmatrix} + \begin{bmatrix} \mathbf{K}_{uu} & \mathbf{K}_{u\theta} \\ \mathbf{0} & \mathbf{K}_{\theta\theta} \end{bmatrix}\begin{Bmatrix} \mathbf{U} \\ \Theta \end{Bmatrix} = \begin{Bmatrix} \mathbf{F}_u \\ \mathbf{F}_\theta \end{Bmatrix} \tag{20}$$

where $\mathbf{M}_{uu}$, $\mathbf{K}_{uu}$, $\mathbf{K}_{\theta\theta}$ and $\mathbf{C}_{\theta\theta}$ are usual global mass, stiffness, conductivity and capacity matrices, and $\mathbf{K}_{u\theta}$ and $\mathbf{C}_{\theta u}$ are coupling matrices combining the mechanical and thermal parts, $\mathbf{U}$ and $\boldsymbol{\Theta}$ are global vectors of nodal displacements and nodal temperatures, respectively, and dots over them correspond to the time derivatives of these vectors. The vectors $\mathbf{F}_u$ and $\mathbf{F}_\theta$ are global vectors of mechanical and thermal forces.

Further the system of coupled equations (20) is reduced to a system of nonlinear algebraic equations through temporal discretization. In this regard, the solution time interval should be developed by a series of time increments $\Delta t = t^{n+1} - t^n$ such that $t = \bigcup_{n=0}^{N-1}[t^n, t^{n+1}]$. A general form of the fully discretized system (20) at each time step Δt can be represented by an equation joining together the mechanical and thermal parts:

$$\mathbf{M}\ddot{\mathbf{d}}^{t+\Delta t} + \mathbf{C}\dot{\mathbf{d}}^{t+\Delta t} + \mathbf{K}\mathbf{d}^{t+\Delta t} = \mathbf{F}^{t+\Delta t} \tag{21}$$

where $\mathbf{M}$, $\mathbf{C}$ and $\mathbf{K}$ are mass, damping and stiffness matrices, which are partitioned matrices combining the corresponding matrices of mechanical and thermal parts, $\mathbf{d}$ is a combined vector of global nodal displacements and temperatures and the time derivatives of this vector, and $\mathbf{F}$ is a global thermal-mechanical force vector.

With a certain time marching scheme, if a solution is known at time $t = t^n$, the system (21) finds the solution at $t = t^{n+1}$, Herewith, because the coupling between mechanical and thermal fields occurs at each time step, the mechanical equation is solved taking into account the actual temperature, and the solution of the thermal equation accounts for the actual displacement. The solution at $t = t^{n+1}$ can be achieved using the iterative Newton-Raphson method. Thus, the system of equations (21) should be rearranged into the linearized form as [33]:

$$\mathbf{R}(\mathbf{d}_i^{n+1}, t^{n+1}) = -\frac{\partial \mathbf{R}(\mathbf{d}_i^{n+1}, t^{n+1})}{\partial \mathbf{d}_i^{n+1}} \Delta \mathbf{d}, \tag{22}$$

which is followed by the update as follows:

$$\mathbf{d}_{i+1}^{n+1} = \mathbf{d}_i^{n+1} + \Delta \mathbf{d}. \tag{23}$$

Here the superscript 'n' represents a discrete time instant and the subscript 'i' denotes an iteration, $\Delta\mathbf{d}$ is a difference between an approximate solution and the exact one of the system (or a correction), $\mathbf{R}$ is a residual, which is a function of the vector of unknowns and the current instant of time. In the case of an implicit time integration algorithm adopted, the residual in (22) can be written in the following general form [34]:

$$\begin{aligned}\mathbf{R}(\mathbf{d}^{n+1}, t^{n+1}) = &\frac{1}{\gamma_1 \Delta t^2}\mathbf{M}\mathbf{d}^{n+1} + \frac{1}{\gamma_2 \Delta t}\mathbf{C}\mathbf{d}^{n+1} + \\ &\mathbf{K}(\mathbf{d}^{n+1}, t^{n+1})\mathbf{d}^{n+1} - \mathbf{F}(\mathbf{d}^{n+1}, t^{n+1})\end{aligned} \tag{24}$$

By decomposing the generalized unknowns $\mathbf{d} = \{\mathbf{U}_u, \mathbf{U}_\theta\}^T$ and the residual forces $\mathbf{R} = \{\mathbf{R}_u, \mathbf{R}_\theta\}^T$ we can rewrite the system (22) as follow:

$$\begin{bmatrix} \hat{\mathbf{K}}_{uu} & \hat{\mathbf{K}}_{u\theta} \\ \hat{\mathbf{K}}_{\theta u} & \hat{\mathbf{K}}_{\theta\theta} \end{bmatrix} \begin{Bmatrix} \Delta\mathbf{U}_u \\ \Delta\mathbf{U}_\theta \end{Bmatrix} = \begin{Bmatrix} \mathbf{R}_u \\ \mathbf{R}_\theta \end{Bmatrix}. \tag{25}$$

In (25) $\hat{\mathbf{K}}_{IJ}$ are submatrices of the coupled Jacobian matrix including the corresponding matrices in (19), $\Delta\mathbf{U}_u$ and $\Delta\mathbf{U}_\theta$ are respective corrections referring to the solution vectors for displacements $\mathbf{U}_u$ and temperature $\mathbf{U}_\theta$, respectively. Note that the system Jacobian matrix is nonsymmetric Therefore, the system of linear algebraic equations (22) should be solved using the unsymmetrical matrix storage and solution scheme at each iteration within each time step.

5. Graded finite element

The finite element framework describing a coupled thermo-mechanical problem of an inhomogeneous 2-D body is applied for simulations of FGM plates. The simulations are assumed to be carried out with the ABAQUS/Standard code [31]. In this regard we aim to develop within the package environment a graded finite element incorporating a gradient of material properties into the discretized model of the FGM plate at the size scale of the element.

Let us consider a base element, whose matrices required for an implementation of the element are calculated by expressions in Appendix. Unlike the conventional homogeneous element, where material parameters are constants, the graded element should provide a spatial dependence of the material parameters. This can be achieved by evaluating the integrals over the element area with Gauss quadratures. Because material constants depend on the position within the element, the numerical

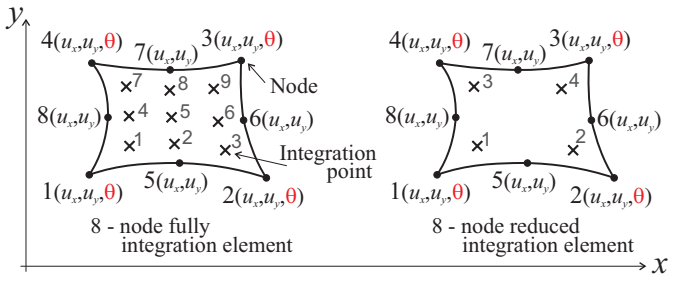

Figure 3: 8-node plane strain thermally coupled element.

integration over the element area assigns different values of the material parameters to the different integration points. Thus, by means of integration of the finite element matrices actual gradients of material properties can be defined within the element. As an example, the Gauss quadrature used for calculations of the stiffness matrix in (A.4) is considered:

$$\mathbf{K}_{uu_{ij}}^{(e)} = \sum_{i=1}^{N}\sum_{j=1}^{N} \mathbf{B}_{u_{ij}}^T \mathbf{D}_{ij} \mathbf{B}_{u_{ij}} J_{ij} w_i w_j. \tag{26}$$

In this expression, i and j are the Gauss points, J_{ij} is the Jacobian and w_i are the Gaussian weights. The matrix $\mathbf{D}$ contains the material constants E and ν depending on the position as shown in (12). Then, the numerical integration samples these coefficients directly at the points i and j of the element. Similarly, other material parameters can be specified within the finite element as a result a continuous variation of the material properties will be introduced into a finite element model.

With this approach at hand we can implement gradients of mechanical material properties into a conventional finite element available in the ABAQUS element library. For this purpose a quadratic eight-node plane strain thermally-displacement coupled element `CPE8T` is used. The finite element exploits a bi-quadratic displacement interpolation and a bi-linear temperature interpolation, i.e. the two-component displacements are given at eight nodes in the displacement-stress analysis, while the temperature is a variable at four corner nodes in the thermal analysis. The element contains the eight Gauss integration points and allows the reduced integration also as shown in Fig. 3.

We elaborate the element stiffness matrix with varying mechanical parameters by means the user-defined material subroutine UMAT. The routine provides an implementation of the incremental form of a user-defined mechanical constitutive law into the code solver and an update of stresses, strains and other solution dependent variables at the Gauss points. Then, the tangential stiffness matrix is specified by the material Jacobian at each material point of the element as

$$\mathbf{J} = \frac{\partial \Delta\boldsymbol{\sigma}}{\partial \Delta\boldsymbol{\varepsilon}}. \tag{27}$$

In the case of a plane strain analysis, the increment of in-plane stresses $\Delta\boldsymbol{\sigma} = (\Delta\sigma_{11}, \Delta\sigma_{22}, \Delta\sigma_{33}, \Delta\sigma_{12})^T$ relates to the incre-

ment of in-plane strains $\Delta\boldsymbol{\varepsilon} = (\Delta\varepsilon_{11}, \Delta\varepsilon_{22}, 0, \Delta\varepsilon_{12})^T$ in accordance with (5) and takes the following matrix form:

$$\Delta\boldsymbol{\sigma} = \mathbf{D}\Delta\boldsymbol{\varepsilon} - \boldsymbol{\beta}\Delta\theta, \tag{28}$$

where the matrix of material constants and the matrix of thermal coefficients are defined by:

$$\mathbf{D} = \bar{E}\begin{bmatrix} 1-\nu & \nu & \nu & 0 \\ \nu & 1-\nu & \nu & 0 \\ \nu & \nu & 1-\nu & 0 \\ 0 & 0 & 0 & \dfrac{1-2\nu}{2} \end{bmatrix}, \boldsymbol{\beta} = \bar{\beta}\begin{bmatrix} 1 \\ 1 \\ 1 \\ 0 \end{bmatrix}. \tag{29}$$

Here, we denote $\bar{E} = \dfrac{E}{(1+\nu)(1-2\nu)}$ and $\bar{\beta} = \dfrac{\beta(1+\nu)}{(2-\nu)}$. Therefore, by programming spatially dependent material parameters $E(\mathbf{x})$, $\nu(\mathbf{x})$ and $\beta(\mathbf{x})$ with functions given in (12) or with any other functional relations, if required, the gradients of these mechanical material properties are incorporated into the element matrices $\mathbf{K}^{(e)}_{uu}$ and $\mathbf{K}^{(e)}_{u\theta}$.

The inhomogeneous properties of the material are entered into the thermal problem by means of the user-defined subroutine UMATHT. The subroutine provides a functional variation of the thermal coefficients $\kappa(\mathbf{x})$ and $c_v(\mathbf{x})$ by sampling them at the Gauss points of the element. In the thermal analysis, the code passes a temperature field and a spatial gradient of temperature in the subroutine, whereas the internal energy $\mathcal{E}$ per unit mass and its derivative with respect to the temperature as well as the heat flux q_i and its derivatives respective to the temperature and the temperature gradient are computed at each integration point of the element in the subroutine. In doing so, it is assumed that the heat flux does not depend on the temperature, but it does the temperature gradient, i.e. the following equalities take place:

$$\frac{\partial q_i}{\partial\theta} = 0 \text{ and } \frac{\partial q_i}{\partial\theta_{,i}} \equiv -\kappa(\mathbf{x}). \tag{30}$$

The internal energy is updated at each time step and its increment is calculated as

$$\Delta\mathcal{E} = c_v(\mathbf{x})\Delta\theta, \text{ where } c_v(\mathbf{x}) \equiv \frac{\partial\mathcal{E}}{\partial\theta}. \tag{31}$$

Therefore, by programming the thermal conductivity and the specific heat as functions of coordinates, the gradation of the thermal properties will be completely defined within the element matrices $\mathbf{K}^{(e)}_{\theta\theta}$ and $\mathbf{C}^{(e)}_{\theta\theta}$.

Additional thermo-mechanical coupling defined by $\mathbf{C}^{(e)}_{\theta u}$ is realized by computing the matrix as a rate of the mechanical energy and storing its value at the Gauss points. Then, the rate of internal energy including a contribution from the mechanical equation pass into the thermal equation as an input rate of energy. Since the thermal and mechanical equations are resolved simultaneously at every solution increment of the coupled thermo-mechanical problem, this contribution of the mechanical equation into the energy balance is accumulated with time.

In should be noted that all forthcoming calculations are performed in the case of static mechanical equilibrium, i.e. inertial forces are neglected in (20). Thus, the spatial variation of the mass density has been set in the graded finite element via the user subroutine USDFLD, defining any field variable at either element nodes or Gauss points.

6. Validation of graded finite element

Analytical solutions known in the literature for FGM plates are used as a reference to verify the graded finite element developed here by means of the mentioned user-defined subroutines in the ABAQUS code. Moreover, with these examples the advantage of using the graded element is illustrated by comparing results obtained with the graded elements with those found with conventional homogeneous elements in the layered approach.

6.1. Element performance for mechanical problems

First, for the sake of verification of the tangential stiffness matrix programmed via the UMAT subroutine we consider a functionally graded isotropic plate in plane strain state subjected to either a uniform displacement or traction, or a bending load perpendicular to the material gradient directed along the x-direction, as shown in Fig. 4. An exponential variation of the Young's modulus along the x-direction as $E(x) = E_1 e^{\gamma x}$, but constant the Poisson's ratio $\nu = 0.3$ are adopted.

The parameter γ in the exponential law is defined by

$$\gamma = \frac{1}{w}\ln\left(\frac{E_2}{E_1}\right), \text{ where } E_1 = 1 \text{ and } E_2 = 8.$$

A general form of the analytical far-field solutions for a nonzero stress, and a displacement and stress of such plate under assumptions of its infinite length and finite width have been derived in [3] and [14], respectively. In the case of the uniform displacement load (Fig. 4b) the analytical formulae for calculating the stress and displacement are as follows:

$$\sigma_{yy}(x) = E^*\varepsilon_0 e^{\gamma x}$$

and

$$u_x(x,y) = -\frac{\nu}{1-\nu}\varepsilon_0 x,$$

where $E^* = \dfrac{E_1}{(1-\nu^2)}$ and $\varepsilon_0 = \dfrac{u_0}{h}$.

The stresses and displacements under uniform tension and bending loads (Fig. 4c and d) can be found from the expressions:

$$\sigma_{yy}(x) = E^* e^{\gamma x}(A_i x + B_i)$$

and

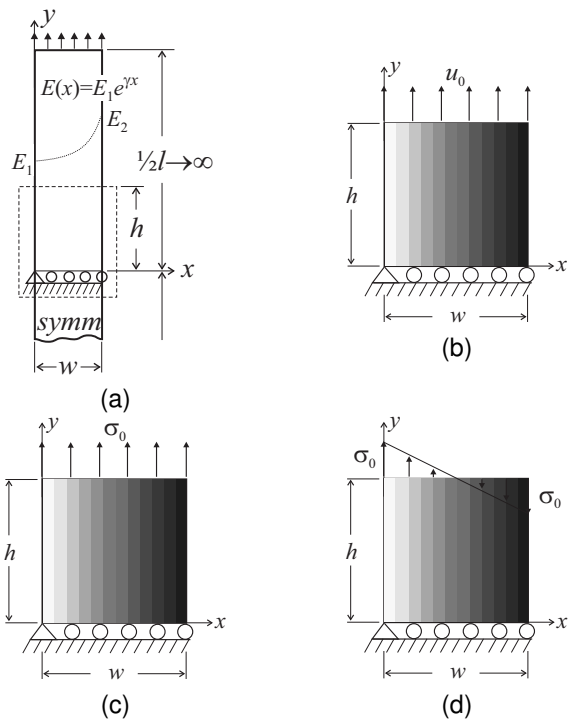

Figure 4: Functionally graded plate: a) geometry; b) uniform displacement perpendicular to the material gradient; c) uniform tension perpendicular to the material gradient; and d) bending perpendicular to the material gradient.

$$u_x(x,y) = -\frac{\nu}{1-\nu}(A_i x^2 + B_i x) - \frac{A_i}{2}x,$$

where $i = t, b$ refer to tension and bending, respectively.

The unknown coefficients are determined in accordance with appropriate loading conditions on the plate boundary such as

$$\int_0^w \sigma_{yy} dx = N \text{ and } \int_0^w \sigma_{yy} x dx = M,$$

where $N = \sigma_0 w$ and $M = \dfrac{\sigma_0 w^2}{6}$. Hence, we have derived the coefficients in the following form:

$$A_t = \frac{\gamma N}{2E^*}\frac{2c_1\gamma - c_2 w\gamma^2}{c_1^2 - c_2(c_3 - 2c_1)},$$
$$B_t = \frac{\gamma N}{2E^*}\frac{c_1 w\gamma - 2(c_3 - 2c_1)}{c_1^2 - c_2(c_3 - 2c_1)}$$

and

$$A_b = \frac{\gamma M}{E^*}\frac{-c_2\gamma}{c_1^2 - c_2(c_3 - 2c_1)},$$
$$B_b = \frac{\gamma M}{E^*}\frac{c_1}{c_1^2 - c_2(c_3 - 2c_1)},$$

where $a = w\gamma$ and $c_1 = ae^a - e^a + 1$, $c_2 = e^a - 1$ and $c_3 = a^2 e^a$.

In the finite element calculations a rectangular FGM plate of width $w = 8$ and a finite length $2h = 16$ is modelled (Fig. 4a). The finite element model is created using symmetry conditions as a result a half of the plate is considered. Either a uniform unit displacement u_0 or a uniform unit traction σ_0 or a bending moment caused by a unit force are applied to the top edge perpendicular to the material gradation, while the boundary displacements are prescribed on the bottom edge, as shown in Fig. 4b-d. Because only mechanical loading is applied, the mechanical part of the system of equations (20) is solved by neglecting the inertia and body forces in the calculations. Thus, a general linear static stress analysis with the user-defined Young's modulus in (29) is carried out. The mesh built for the plate model has 16 graded elements, while both 16 and 64 second-order homogeneous plane strain quadrilateral elements `CPE8` is adopted in the case of the layered models created as well.

The distributions of stress σ_{yy} and displacement u_x over the plate width at the ordinate $y = 0$ are compared in Figs. 5-7 between the analytical solutions and the results calculated by using the layered finite element models and the graded finite element. A very good agreement between the analytical solutions and the numerical results following from the use of the developed graded element are obvious for both displacement and stress in all considered cases of loading. The solutions with graded element match the analytical ones with small differences due to the finite length of plate in the simulations. At the same time the model based on layers of homogeneous elements produces a stepwise stress field and the stress jumps increase with increasing the coordinate of the gradation direction. To improve the accuracy in this case, a finer mesh is required (illustrated by the dotted lines with rhombuses in Figs. 5-7), in turn, it leads to a sufficient increase in the computational cost, namely, 0.7 CPU time in seconds for the layered model against 0.2 for the model with the graded elements. Although the displacements predicted by both the graded element and the layered model are close to each other and are in a good accordance with the analytical solutions. The results presented above are consistent with those known in [14] and [19].

6.2. Element performance for thermal problems

The next example concerns the implementation of graded thermal properties into the finite element. For this purpose an analytical solution obtained in [20] for the transient thermal response of a FGM plate shown in Fig. 8a is used for comparison. The plate considered in the example presents an equivalent 2-D model of a cube which is subjected to prescribed temperatures on the left and right sides, while is insulated on the top and bottom sides. It is assumed that in the plate the thermal conductivity and the specific heat vary along the x-direction as exponential functions defined by expressions:

$$\kappa(x) = \kappa_0 e^{2\zeta x} \text{ and } c(x) = c_0 e^{2\zeta x},$$

where κ_0=5, c_0=1 and ζ=3 according with the data in [20].

The exact solution of this problem is given by:

$$\theta(x,t) = T_L\frac{1 - e^{-2\zeta x}}{1 - e^{-2\zeta L}} + \sum_{n=1}^{\infty} B_n \sin(\frac{\pi n x}{L}) e^{-\zeta x} e^{(\frac{-\pi^2 n^2}{L^2} + \zeta^2)\epsilon t},$$

where

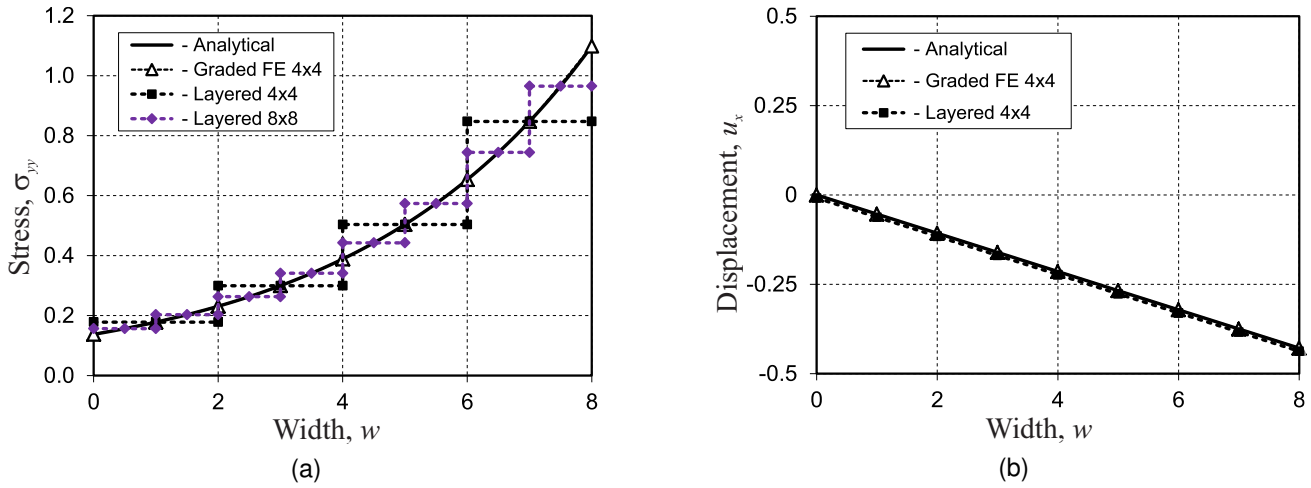

Figure 5: Uniform displacement applied perpendicular to the material gradient: a) the distribution of stress σ_{yy}; and b) the distribution of displacement u_x.

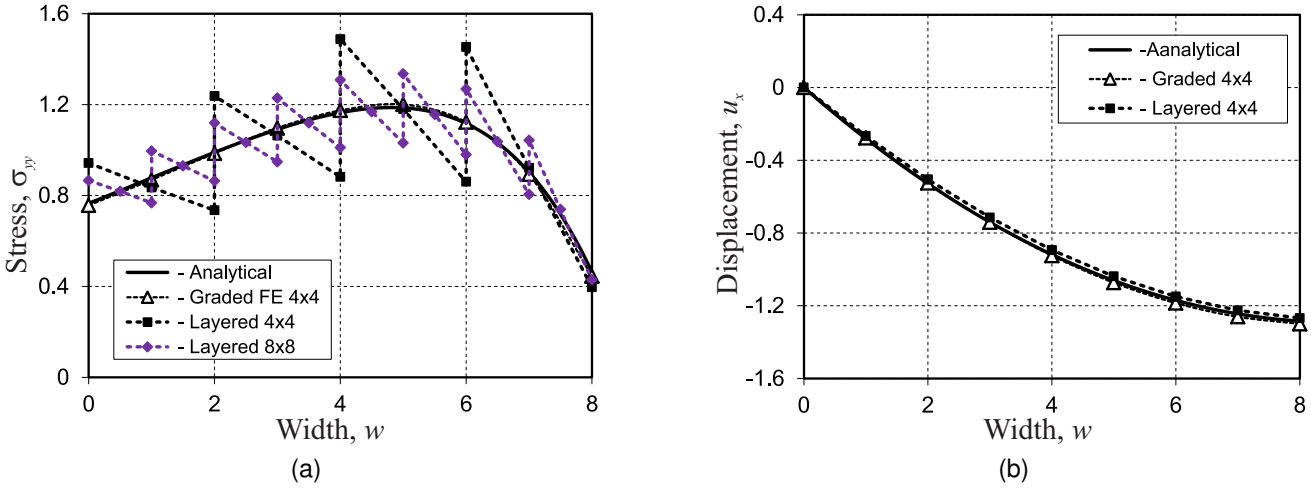

Figure 6: Uniform tension load applied perpendicular to the material gradient: a) the distribution of stress σ_{yy}; and b) the distribution of displacement u_x.

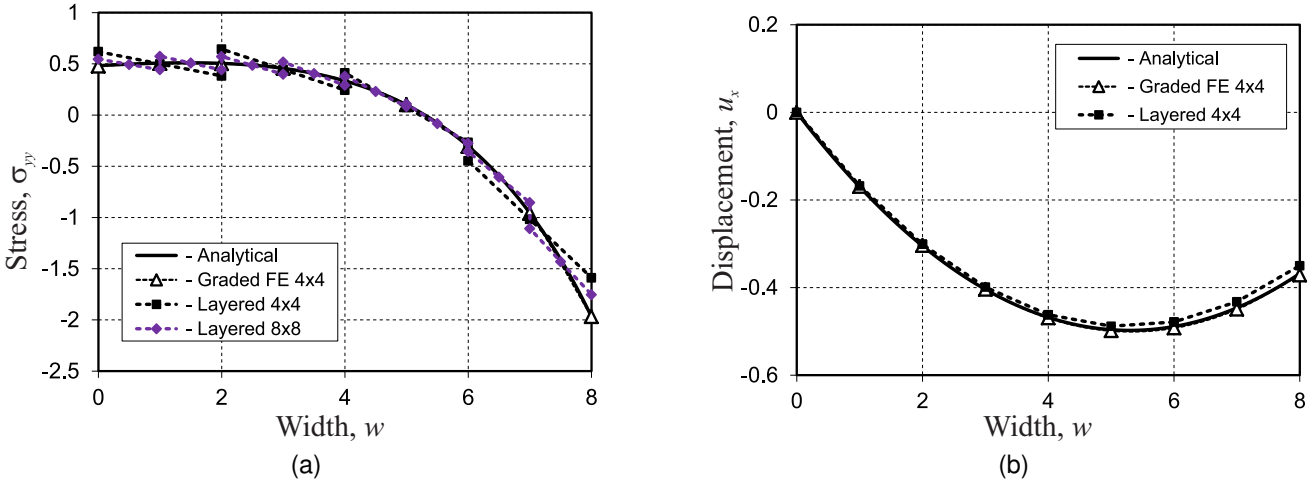

Figure 7: Bending load applied perpendicular to the material gradient: a) the distribution of stress σ_{yy}; and b) the distribution of displacement u_x.

$$B_n = -T_L \frac{2e^{\zeta L}}{\zeta^2 L^2 + \pi^2 n^2} \left[\zeta L \sin(\pi n) \frac{1 + e^{-2\zeta L}}{1 - e^{-2\zeta L}} - \pi n \cos(\pi n) \right].$$

In the finite element simulations only the thermal equation of the coupled thermo-mechanical system of equations (20) is solved in this case. Thus, a transient heat transfer analysis is performed with ABAQUS, calling the material subroutine UMATHT only. The mesh of 10×10 of the graded finite elements is employed in the analysis to provide a time step of $t = 0.001$ required for comparisons. The results of comparisons between the analytical and numerical solutions of the transient temperature field at different moments of time are presented in Fig. 8b.

In the plot, the lines of different styles illustrate the analytical solutions, while the markers show the finite element predictions. It can be seen that there is an excellent agreement between the analytical and numerical results.

6.3. Element performance for steady thermoelasticity problems

To evaluate the performance of the graded element for predictions of thermo-mechanical problems, a steady state thermoelasticity analysis of a FGM plate shown in Fig. 1 is carried out. A closed-form solution of this problem is available in [3]. In that study a plate of an infinite length is considered. It was assumed an exponential variation of Young's modulus, thermal conductivity and specific heat along the width of the plate. They are defined as the following functions of the x-coordinate:

$$E(x) = E_1 e^{\gamma x}, \text{ where } \gamma w = \ln\left(\frac{E_2}{E_1}\right) = 0.37498$$

$$\alpha(x) = \alpha_1 e^{\eta x}, \text{ where } \eta w = \ln\left(\frac{\alpha_2}{\alpha_1}\right) = 0.51283$$

$$\kappa(x) = \kappa_1 e^{\zeta x}, \text{ where } \zeta w = \ln\left(\frac{\kappa_2}{\kappa_1}\right) = 2.5014$$

where E_1, α_1, κ_1 and E_2, α_2, κ_2 are the material parameters given on the sides of FGM plate at $x = 0$ and $x = w$, respectively. The Poisson's ratio is taken as a constant value of 0.25. As boundary conditions, the prescribed temperatures are given on the plate surfaces: $T_1 = T(x = 0)$ and $T_2 = T(x = w)$.

General expressions of the steady state temperature field $\theta(x)$ and the respective thermally-induced stress σ_{yy} can be found in [3]. Their explicit forms corresponding to the actual material gradations are deduced herein and can be written as follows:

$$\theta(x) = T_1 + (T_2 - T_1) \frac{e^{-\zeta x} - 1}{e^{-\zeta w} - 1}$$

and

$$\sigma_{yy}(x) = E_*(x) e^{\gamma x} \left[(Ax + B) - \alpha_*(x) e^{\eta x} \left(C + D(e^{-\zeta w} - 1) \right) \right],$$

where $E_*(x) = \dfrac{E(x)}{1 - \nu^2}$ and $\alpha_*(x) = (1 + \nu)\alpha(x)$. Also we denote that $C = (T_1 - T_0)$ and $D = \dfrac{T_2 - T_1}{e^{-\zeta w} - 1}$. The coefficients A and B can be derived by using the conditions of an unconstrained boundary, i.e.

$$\int_0^w \sigma_{yy} dx = 0 \text{ and } \int_0^w \sigma_{yy} x dx = 0.$$

They are not presented here because of their cumbersome forms.

A FGM plate with dimensions of $w = 1$ and $2l = 2$ of non-dimensional units as shown in Fig. 1 is considered. Due to symmetry, half of the plate is meshed. The finite element model used is composed of 100 graded elements in a mesh 10×10. To compare the analytical and finite element results, we use the same input values as given in [3]. It is assumed that the plate is stress free under temperature T_0 of 10. Firstly, the plate is subjected to thermal loading such that the temperature of the right plate surface T_2 is held at T_0, while the temperature of its left surface T_1 is variable. The ratio T_1/T_0 takes values of 5, 10 and 20. In the other case the temperature of the right plate surface is assumed lower than the temperature T_0 and is maintained at the constant value of $T_2 = 0.5T_0$, but the temperature of the left surface T_1 is changeable such that the ratio T_1/T_0 is of 0.5, 0.2, 0.1 and 0.05.

A steady state analysis of the thermo-mechanical problem can be performed by using a simplified two-step or sequential temperature-stress analysis, i.e. a steady temperature field is firstly determined from the heat transfer equation (14) at appropriate thermal boundary and initial conditions. This is followed by solving the displacements and stresses induced by the temperature gradient calculated from the mechanical equation (13) under given mechanical boundary and initial conditions. In this case, the system of the governing equations (21) is supposed to be fully uncoupled. Hence, the system of algebraic equations (26) is significantly simplified due to the zero coupled submatrices of the Jacobian matrix, as a result the computational cost of this analysis is not high. Both analyses are performed using the same meshes. The gradients of thermal and mechanical properties are incorporated into the graded element by programming the user-defined subroutines in accordance with the data given in [3].

The distributions of temperature and thermally-induced stress computed analytically and numerically with the graded element are compared in Figs. 9 and 10. All plots are presented along the x-axis of the symmetry line at $y = 0$. In the plots the lines refer to the analytical solutions, whereas the markers correspond to the results of the finite element analysis. Fig. 9 shows the comparisons for the first case of thermal loading. One can see that there is an excellent agreement between the results. Small differences between the stress solutions can be explained by the finite length of the plate used in the finite element analysis, because the mesh refinement does not improve the results. Fig. 10 illustrates similar comparisons for temperature fields and related thermal stresses obtained for the second case of thermal loading. These graphs also clearly demonstrate that the finite element solutions are in very good accordance with the analytical ones.

The contour plots of the stress distribution σ_{yy} for the two different cases of thermal loading considered above are also pre-

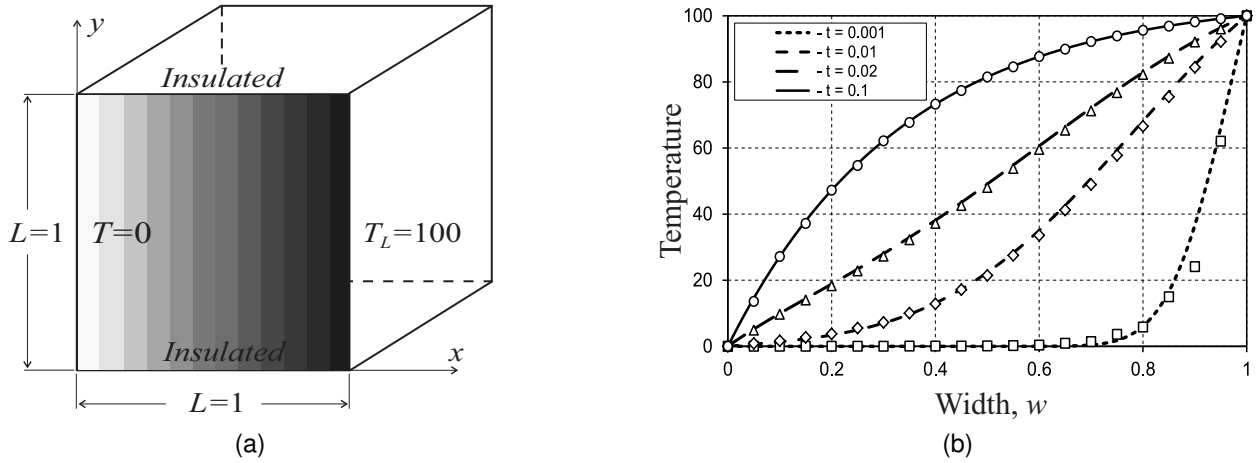

Figure 8: Transient heat conduction in the FGM plate [20]: a) geometry and BCs of the 2-D model; and b) distributions of the temperature with time along the plate width w, calculated on the mesh 10×10.

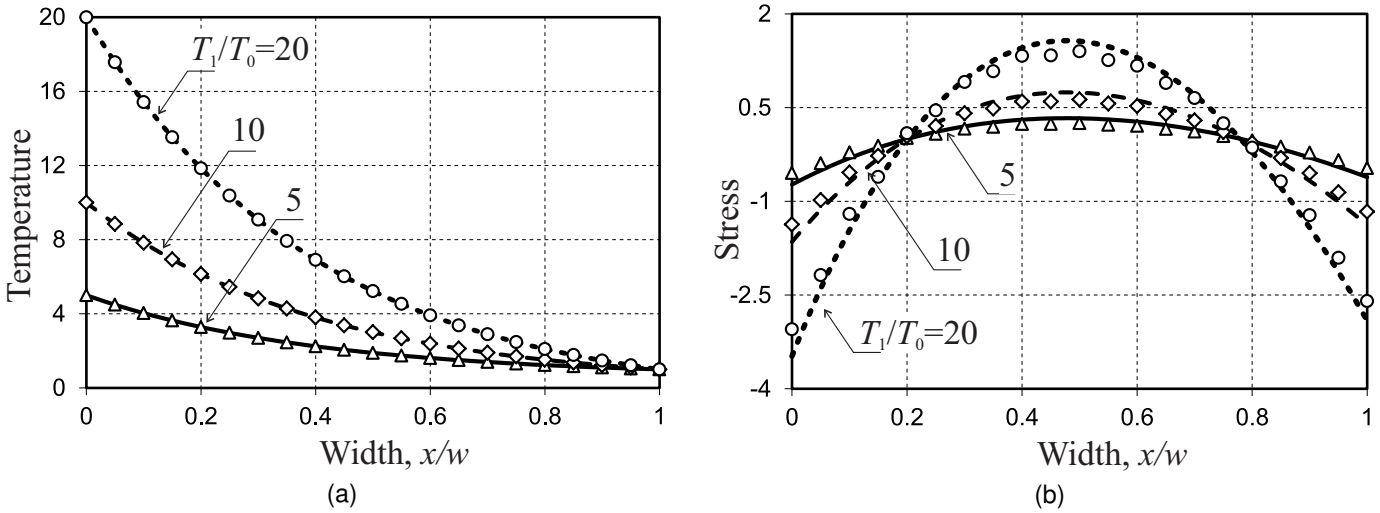

Figure 9: Comparisons of steady state solutions for $T_2 = T_0$: a) temperature distributions normalized by T_0; and b) stress σ_{yy} distributions normalized by $\sigma_0 = E_1\alpha_1 T_0/(1-\nu)$.

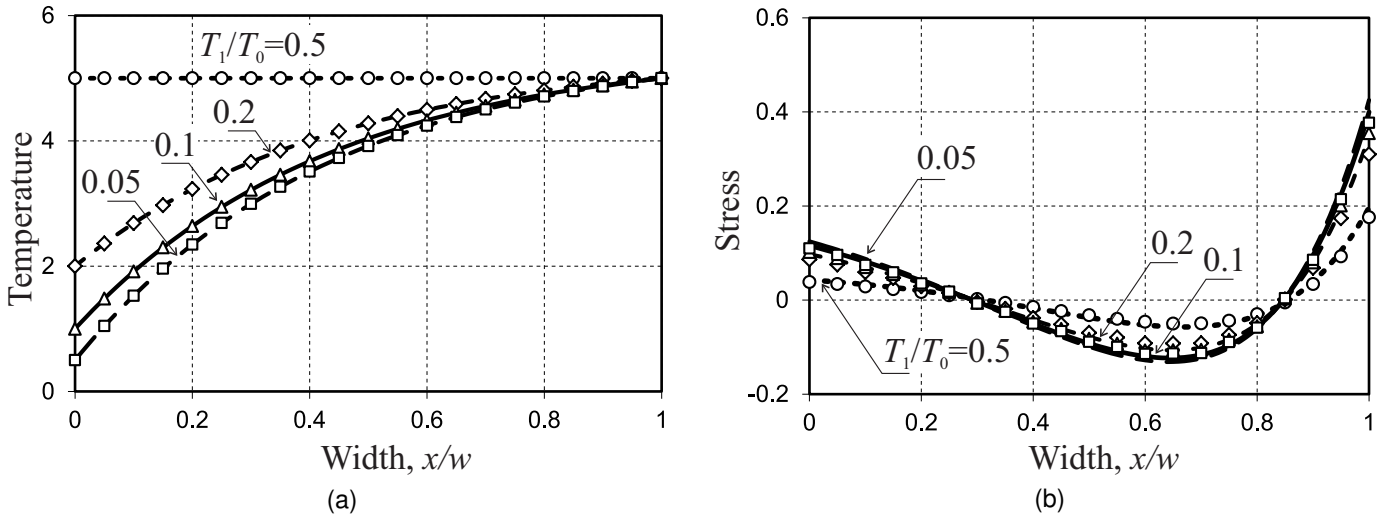

Figure 10: Comparisons of steady state solutions for $T_2 = \frac{1}{2}T_0$: a) temperature distributions normalized by T_0; and b) stress σ_{yy} distributions normalized by $\sigma_0 = E_1\alpha_1 T_0/(1-\nu)$.

sented in Fig. 11. One can see from Fig. 11a that the highest tensile stress occurs mainly in the middle portion of the plate, while the highest compressive stress takes place near the edges of the plate under thermal loading conditions at $T_2 = T_0$ and variety of ratios T_1/T_0. In contrast, the applied temperature $T_2 = 0.5T_0$ at different ratios of T_1/T_0 induces the highest tensile stress close to the plate edges, but the compressive stress appears to be high in the middle of the plate as was shown in Fig. 11b.

6.4. Element performance for transient thermoelasticity problems

Finally, the accuracy of the proposed graded finite element is validated from the standpoint of simulations of coupled thermo-mechanical analyses. To estimate the quality of predictions with this element, the finite element solution available in [10] for the FGM plate presented in Section 3 is used as a basis of comparisons. The metal/ceramic plate of length $2l = 100$mm and width $w = 10$mm as shown in Fig. 1 is considered. The material properties of constituents are listed in Table 1 and vary in the x-direction in accordance with functions in (12). Note that unlike the foregoing analyses in the current analysis the Poisson's ratio and the mass density are functions of the x-coordinate within the graded element also.

One cycle of thermal shock is applied to the FGM plate as a thermal load. It is assumed that the functionally graded plate is suddenly heated from the initial temperature T_0=300K to the temperature T_H=1300K on the ceramics surface, while the temperature T_L=300K is maintained on the metal surface. After a while, when a steady state is achieved in the plate, the ceramic surface of the plate is quickly cooled to the initial temperature T_0 =300K, as shown in Fig. 12.

The simulation procedure of the FGM plate subjected to thermal shock is conventionally divided into two processes such as heating and cooling. Under heating the transient thermo-mechanical task with given thermal boundary conditions, namely, the prescribed temperature $T = T_H$ at $x = 0$ and the known temperature $T = T_L$ at $x = w$ is to be solved. The analysis should be terminated when the temperature field within the plate reaches the steady state. This problem is similar to the previous one considered in Subsection 6.3 and can be simulated via the sequentially coupled thermal-stress analysis to obtain the steady state solution. Once the steady distributions of the temperature and the associated thermal stresses throughout the domain of FGM plate due to heating are known, the transient solution of thermo-mechanical problem with forced convection on the ceramic surface at $x = 0$ should be undertaken to model cooling of the plate. In this case a fully coupled thermal-stress analysis is employed, i.e. the equations of motion and energy balance in (20) are resolved simultaneously at each time increment. Thus, the Jacobian matrix in (25) is fully filled and nonsymmetric that leads to using computationally expensive procedures to find the temperature-stress solution. The heat equation in (20) is supplemented by a given convection boundary condition (10_4) as well, where the film convection coefficient is h=2000 W/mm^{2}K and the temperature of a surrounding medium is T_∞=300K.

The accuracy of calculations strongly depends on a chosen time increment, which is selected based on a prescribed maximum allowable nodal temperature change in this increment and a size of a typical element in mesh. In the calculations, to avoid spurious oscillations and convergence problems arising from incompatibility between the minimum usable time increment Δt and the typical element size Δl, we construct the mesh with elements satisfying the following relationship [31]:

$$\Delta t \geq \frac{\rho c_v}{6\kappa}\Delta l^2.$$

Because of comparisons with the results in [10] we required a very small time increment of the order $10^{-4}s$ in simulations. Hence, following the above mentioned criterion, a finer mesh with a typical element size of order 10^{-2}mm is used. The mesh contains of 34920 graded elements and 35295 nodes. A restart option available in ABAQUS is utilized to speed up the analysis. We run the next sub-analyses with time increments increased in a needed number times. In doing so each analysis is calculated in 100 steps with a fixed time increment value. The total analysis of the FGM plate was completed for 2 hours on a personal computer with Intel(R) Core(TM) i7-3770 CPU 340GHz.

The distributions of temperature and thermally-induced stresses within the FGM plate arising from heating and fast cooling on the ceramic surface are compared in Figs. 13-15 between the finite element solutions published in [10] and those obtained in the present study. In the plots the lines relate to the present solutions, whereas the markers show the results known in the literature. It is obvious from the figures that the both finite element solutions qualitatively are complete match each other for the distributions of temperature and stress. There are some small quantitative difference between them that may be referred to an incomplete input information taken from [10] or due to an inaccuracy in the digitization of the respective graphs there. The steady state temperature field at heating and the transient temperature distributions due to cooling have somewhat lower values in the middle part of the plate in the present study than in the published paper, Fig. 13. Nevertheless, the peaks of thermally-induced stresses and the distributions of stress computed for both heating and cooling are in a very good agreement between those two predictions as shown in Fig. 14 and Fig. 15, respectively.

7. Conclusions

Summarizing the results of this study we can conclude the following. A finite element formulation of the coupled thermo-mechanical problem in functionally graded plates undergoing a plane strain condition has been presented. The theoretical framework presented here has been applied to developing a functionally graded two-dimensional plane strain finite element. The graded element that implements gradients of material properties at the element level into a finite element model of a FGM plate has been incorporated within the engineering finite element package ABAQUS. For this purpose the conventional temperature-displacement plane strain finite element `CPE8T`

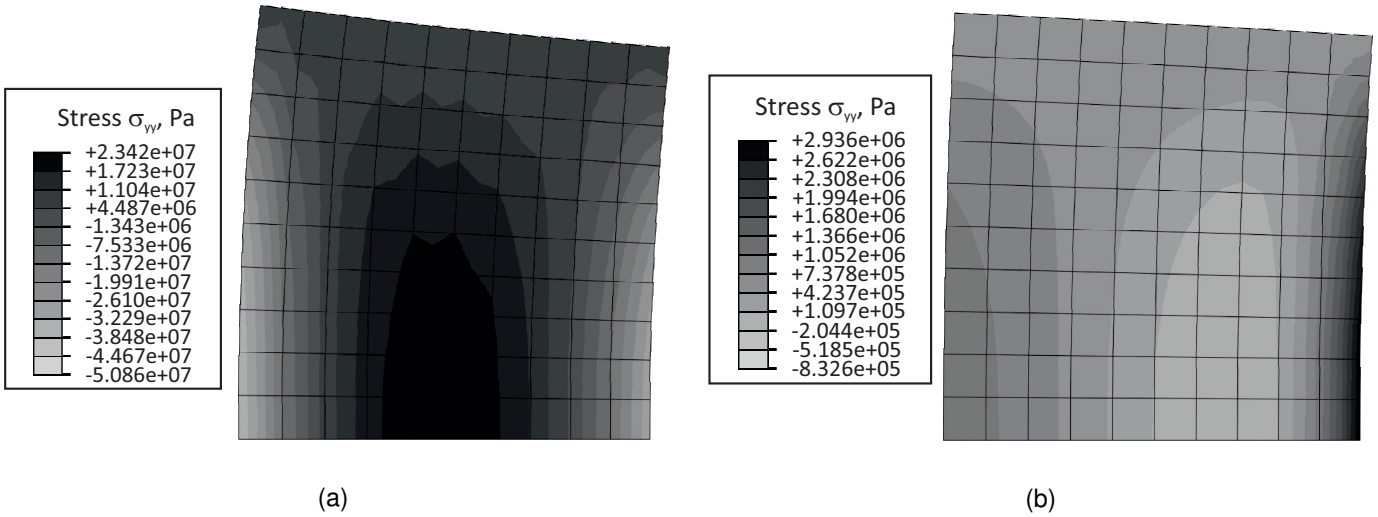

Figure 11: Contour plots of stress σ_{yy} at: a) $T_2 = T_0$ and T_1/T_0=20; and b) $T_2 = 0.5T_0$ and T_1/T_0=0.5.

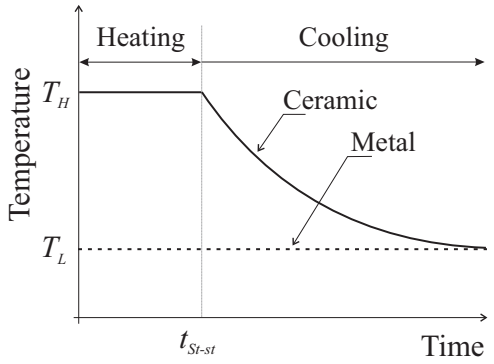

Figure 12: A scheme of thermal shock conditions.

from the ABAQUS library has been endowed by a feature to grade element properties. This has been achieved by programming the user-defined subroutines such as UMAT, UMATHT and USDFLD, which allow the mechanical and thermal material properties programmed as spatially-dependent functions to sample directly at the Gaussian points of the element.

To estimate the accuracy of the graded element developed, respective case studies have been carried out. In this regard different problems including pure mechanical and thermal analyses, and uncoupled and fully coupled analyses of thermo-mechanical problems have been solved. The results obtained with the graded finite element and those known in the literature for the thermo-mechanical analyses of functionally graded plates have been compared. The comparisons showed a very good agreement between them for both the temperature fields and the distributions of thermally-induced stresses. This clearly indicates that the developed finite element model enables to perform accurate and reliable predictions of thermal and mechanical responses of FGM plates.

Acknowledgements

The first author acknowledges the Erasmus Mundus exchange programme ACTIVE (grant No. AC/TG2/SOTON/PD/23/2015) for the financial support of his research in University of Southampton.

Appendix

The matrices presented in the system of equations (20) can be written in explicit forms as follows:

$$\mathbf{M}_{uu}^{(e)} = \int_{\mathcal{A}^{(e)}} \rho(\mathbf{x})\mathbf{N}^T\mathbf{N}d\mathcal{A} \tag{A.1}$$

$$\mathbf{C}_{\theta u}^{(e)} = \int_{\mathcal{A}^{(e)}} T_0\tilde{\mathbf{N}}^T\beta(\mathbf{x})\mathbf{B}_u d\mathcal{A} \tag{A.2}$$

$$\mathbf{C}_{\theta\theta}^{(e)} = \int_{\mathcal{A}^{(e)}} \rho(\mathbf{x})c_v(\mathbf{x})\mathbf{N}^T\mathbf{N}d\mathcal{A} \tag{A.3}$$

$$\mathbf{K}_{uu}^{(e)} = \int_{\mathcal{A}^{(e)}} \mathbf{B}_u^T\mathbf{D}(\mathbf{x})\mathbf{B}_u d\mathcal{A} \tag{A.4}$$

$$\mathbf{K}_{u\theta}^{(e)} = -\int_{\mathcal{A}^{(e)}} \mathbf{B}_\theta^T\beta(\mathbf{x})\tilde{\mathbf{N}}d\mathcal{A} \tag{A.5}$$

$$\mathbf{K}_{\theta\theta}^{(e)} = \int_{\mathcal{A}^{(e)}} \mathbf{B}_\theta^T\kappa(\mathbf{x})\mathbf{B}_\theta d\mathcal{A} \tag{A.6}$$

$$\mathbf{F}_{u}^{(e)} = \int_{\Gamma^{(e)}\in\Gamma_\sigma} \mathbf{N}^T\bar{t}d\Gamma + \int_{\Gamma^{(e)}\in\Gamma_\sigma} \mathbf{N}^T\mathbf{b}d\Gamma \tag{A.7}$$

$$\mathbf{F}_{\theta}^{(e)} = \int_{\Gamma^{(e)}\in\Gamma_q} \tilde{\mathbf{N}}^T\bar{q}d\Gamma + \int_{\Gamma^{(e)}\in\Gamma_q} \tilde{\mathbf{N}}^T\mathcal{R}d\Gamma \tag{A.8}$$

where $\mathbf{B}_u$ and $\mathbf{B}_\theta$ are matrices of gradients of the shape functions and $\mathbf{D}$ is a matrix of the elasticity coefficients.

References

[1] Y. Miyamoto, W.A. Kaysser, B.H. Rabin, A. Kawasaki and R.G. Ford, Functionally Graded Materials Design, Processing and Applications. Springer, Science+Business Media, New York, 1999.

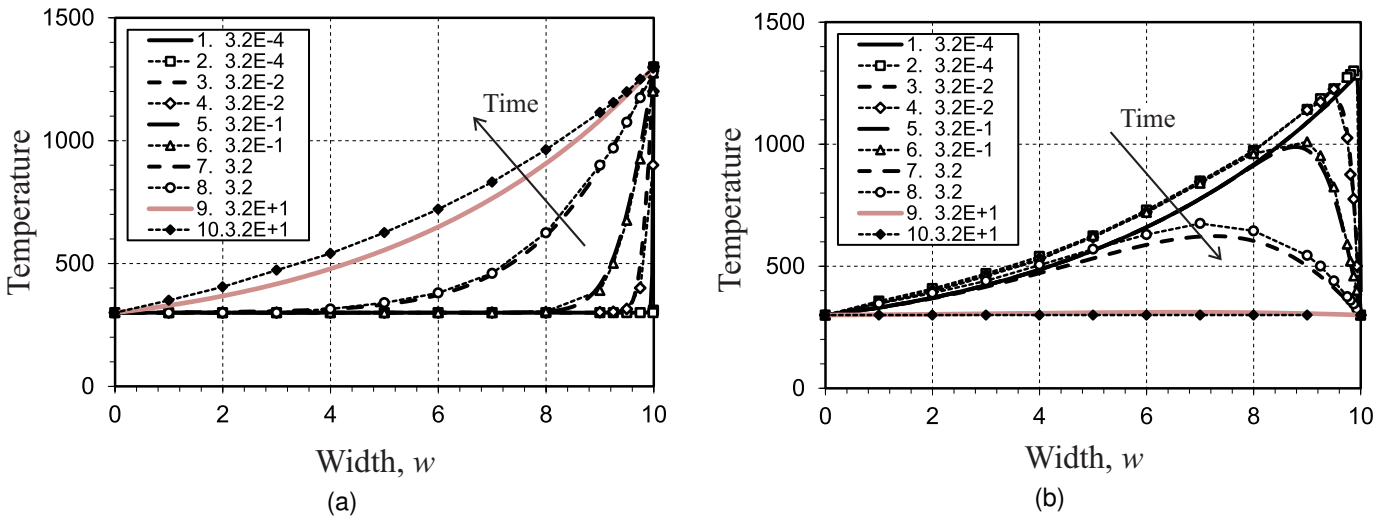

Figure 13: Transient temperature distribution in the FGM plate with volume fraction parameter $p = 1.0$: a) under heating; and b) under cooling.

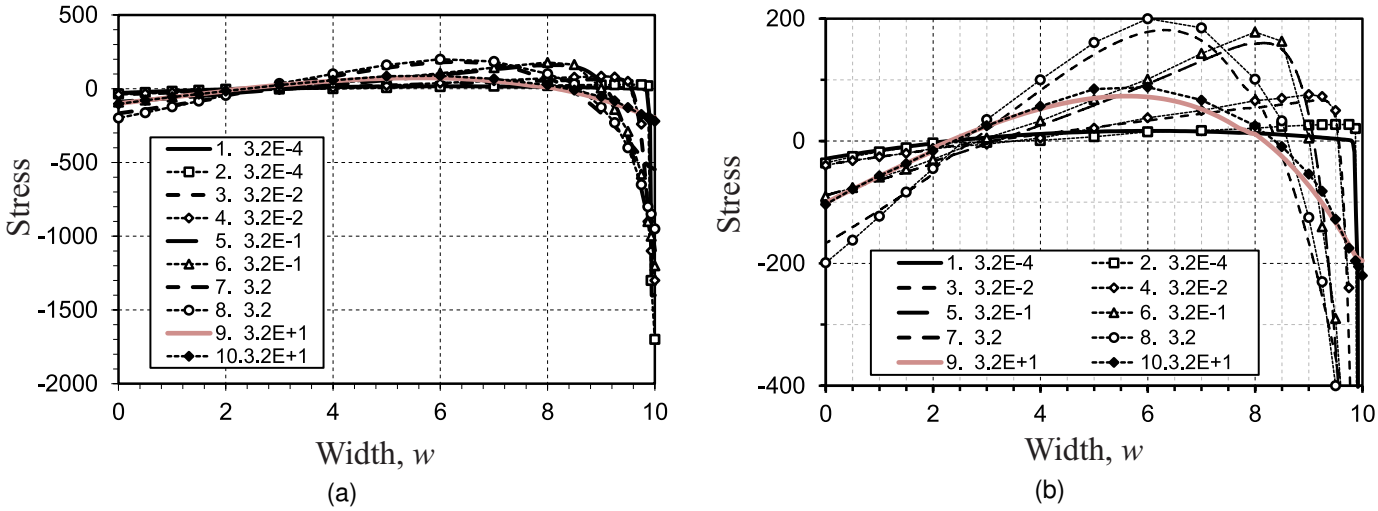

Figure 14: Transient thermally induced stress σ_{yy} in the FGM plate with volume fraction parameter $p = 1.0$ under heating: a) general view; and b) zoomed view.

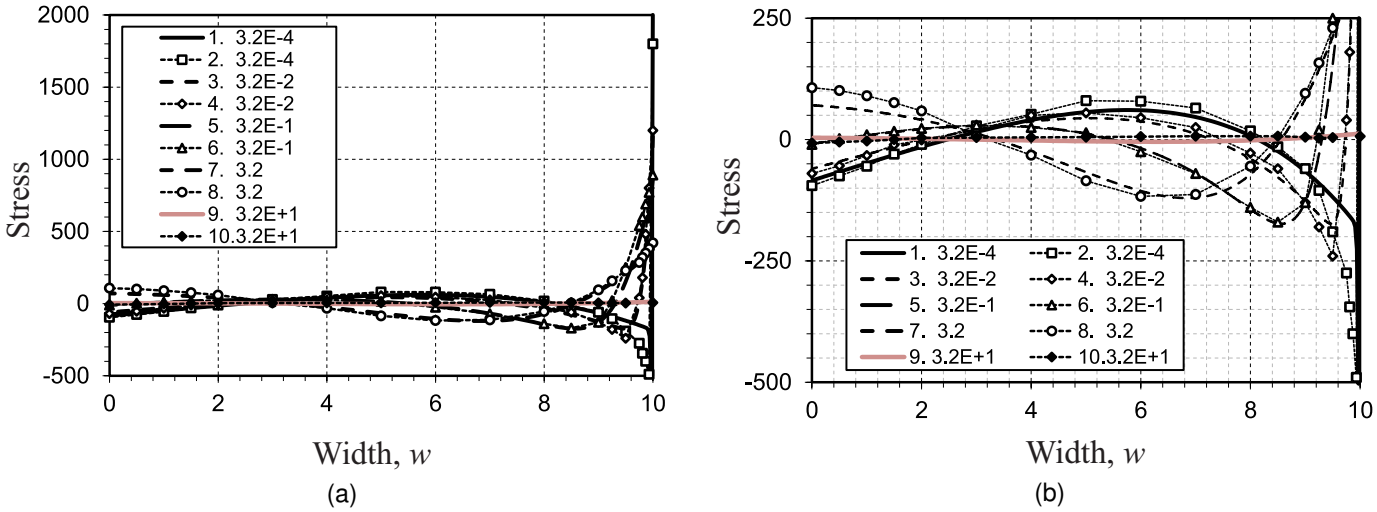

Figure 15: Transient thermally induced stress σ_{yy} in the FGM plate with volume fraction parameter $p = 1.0$ under cooling: a) general view; and b) zoomed view.

[2] A. Kawasaki, R. Watanabe, Thermal fracture behavior of metal/ceramic functionally graded materials. Engineering Fracture Mechanics 69(1416) (2002) 1713–1728.
[3] F. Erdogan, B.H. Wu, Crack problems in FGM layers under thermal stresses. Journal of Thermal Stresses, 19(3) (1996) 237–265.
[4] Z.H. Jin, G.H. Paulino, Transient thermal stress analysis of an edge crack in a functionally graded material. International Journal of Fracture 107 (2001) 73–98.
[5] T. Sadowski, Non-symmetric thermal shock in ceramic matrix composite (CMC) materials. In: Lecture Notes on Composite Materials - Current Topics and Achievements, R. de Borst and T. Sadowski (eds.) Solid Mechanics and its Applications 154, Springer, Science+Business Media, B.V. 2009 pp. 99–148.
[6] L. Marsavina, T. Sadowski, N. Faur, Numerical investigation of the stress field near a crack normal to ceramic-metal interface. Journal of Mechanical Science and Technology, 25(2) (2011) 309–315.
[7] V. Petrova, S. Schmauder, Modelling of thermal fracture of functionally graded/homogeneous bimaterial structures under thermo-mechanical loading. Key Engineering Materials, 592-593 (2014) 145–148.
[8] V. Birman, L.W. Byrd, Modeling and analysis of functionally graded materials and structures, Appl. Mech. Rev 60(5) (2007) 195–216.
[9] H. Altenbach, V.A. Eremeyev, Mechanics of viscoelastic plates made of FGMs. In: Computational Modelling and Advanced Simulations, J. Murin, V. Kompis and V. Kutis (eds.) Computational Methods in Applied Sciences 24. Heidelberg: Springer, 2011 pp. 33–48.
[10] T. Fuchiyama, N. Noda, Analysis of thermal stresse in a plate of functionally gradient material, JSAE Review 16 (1995) 373–387.
[11] G. Anlas, N.H. Santare, J. Lambros, Numerical calculation of stress intensity factors in functionally graded materials. International Journal of Fracture 104 (2000) 131–143.
[12] T. Fujimoto, N. Noda, Influence of the Compositional Profile of Functionally Graded Material on the Crack Path under Thermal Shock. J. Am. Ceram. Soc. 84(7) (2001) 1480–1486.
[13] M.H. Santare, J. Lambros, Use of graded finite elements to model the behavior of nonhomogeneous materials. J. Appl. Mech. 67(4) (2000) 819–822.
[14] J.H. Kim, G.H. Paulino, Isoparametric graded finite elements for nonhomogeneous isotropic and orthotropic materials. J. Appl. Mech. 69 (2002) 502–514.
[15] Y.D. Lee, F. Erdogan, Residual/thermal stresses in FGM and laminated thermal barrier coatings, International Journal of Fracture 69 (1994) 145–165.
[16] B. Chen, L. Tong, Y. Gu, H. Zhang, O. Ochoa, Transient heat transfer analysis of functionally graded materials using adaptive precise time integration and graded finite elements, Numerical Heat Transfer. Part B: Fundamentals 45(2) (2004) 181–200.
[17] C.E. Rousseau, H.V. Tippur, Compositionally graded materials with cracks normal to the elastic gradient, Acta. Mater. 48 (2000) 4021–4033.
[18] P. Gu, M. Dao, R.J. Asaro, A simplified method for calculating the crack tip field of functionally graded materials using the domain integral. Journal of Applied Mechanics 66 (1999) 101–108.
[19] W.G. Buttlar, G.H. Paulino, S.H. Song, Application of graded finite elements for asphalt pavements. J. Eng. Mech. 132(3) (2006) 240–248.
[20] A. Sutradhar, G.H. Paulino, L.J. Gray, Transient heat conduction in homogeneous and nonhomogeneous materials by the Laplace transform Galerkin boundary element method, Eng. Anal. Boundary Elem. 26 (2002) 119–132.
[21] T. Sadowski, P. Golewski, The analysis of heat transfer and thermal stresses in thermal barrier coatings under explotation, Defect and Diffusion Forum 326-328 (2012) 530–535.
[22] T. Sadowski, P. Golewski, Description of mon-stationary heat transfer in two-phase polycrystalline metal-ceramic composites, Acta Physica Polonica A 128(4) (2015) 624–628.
[23] J. Hein, J. Storm, M. Kuna, Numerical thermal shock analysis of functionally graded and layered materials, International Journal of Thermal Science 60 (2012) 41–51.
[24] I.V. Ivanov, T. Sadowski, D. Pietras, Crack propagation in functionally graded strip under thermal shock. The European Physical Journal Special Topics 222 (7) 2013 1587-1595.
[25] T. Sadowski, D. Pietras, I. Ivanov, Estimation of thermal intensity factor in a strip with various property gradations subjected to thermal shock, Key Engineering Materials 601 (2014) 71–75.
[26] P. Liu, T. Yu,T.Q. Bui, C. Zhang, Y. Xu, C.W. Lim, Transient thermal shock fracture analysis of functionally graded piezoelectric materials by the extended finite element method. International Journal of Solids and Structures 51 (2014) 2167–2182.
[27] E. Martinez-Paneda, R. Gallego, Numerical analysis of quasi-static fracture in functionally graded materials, International Journal of Mechanics and Materials in Design 11(4) (2015) 405–424.
[28] V.N. Burlayenko, H. Altenbach, T. Sadowski, S.D. Dimitrova, Computational simulations of thermal shock cracking by the virtual crack closure technique in a functionally graded plate, Computational Materials Science 116 (2016) 11–21.
[29] V.N. Burlayenko, Modelling thermal shock in functionally graded plates with finite element method. Advances in Materials Science and Engineering 2016 (2016), 12 pages.
[30] V.N. Burlayenko, T. Sadowski, FE modeling of delamination growth in interlaminar fracture specimens. Budownictwo i Architektura 2(1) (2008) 95–109.
[31] ABAQUS 6.12 User's Manuals, Dassault Systèmes Simulia Corp., Providence, RI, USA, 2012.
[32] R.B. Hetnarski, M.R. Eslami, Thermal Stresses - Advanced Theory and Applications. Springer, Science+Business Media, B.V., 2009.
[33] K.J. Bathe, M.M.I. Baig, On a composite implicit time integration procedure for nonlinear dynamics. Computer and Structure 83 (2005) 2513–2524.
[34] T. Belytschko, W.K Liu, B. Morgan, Nonlinear Finite Elements for Continua and Structures. John Wiley & Sons Ltd., Chester, UK, 2000.

LaTeX Source Files

Click here to download LaTeX Source Files: Burl_Alt_Sad_Dim_Bhas_R1.tex